

Toward Drug-Target Interaction Prediction via Ensemble Modeling and Transfer Learning

Po-Yu Kao
Insilico Medicine Taiwan Ltd.
Taipei, Taiwan
ken.kao@insilicomedicine.com

Shu-Min Kao
Insilico Medicine Taiwan Ltd.
Taipei, Taiwan
allen.kao@insilicomedicine.com

Nan-Lan Huang
Insilico Medicine Taiwan Ltd.
Taipei, Taiwan
shannon.huang@insilicomedicine.com

Yen-Chu Lin
Insilico Medicine Taiwan Ltd.
Taipei, Taiwan
jimmy.lin@insilicomedicine.com

Abstract—Drug-target interaction (DTI) prediction plays a crucial role in drug discovery, and deep learning approaches have achieved state-of-the-art performance in this field. We introduce an ensemble of deep learning models (EnsembleDLM) for DTI prediction. EnsembleDLM only uses the sequence information of chemical compounds and proteins, and it aggregates the predictions from multiple deep neural networks. This approach not only achieves state-of-the-art performance in Davis and KIBA datasets but also reaches cutting-edge performance in the cross-domain applications across different bio-activity types and different protein classes. We also demonstrate that EnsembleDLM achieves a good performance (Pearson correlation coefficient and concordance index > 0.8) in the new domain with approximately 50% transfer learning data, i.e., the training set has twice as much data as the test set.

Index Terms—drug-target interaction prediction, ensemble modeling, transfer learning, convolutional neural network, deep neural network

I. INTRODUCTION

Drug-target interaction (DTI) prediction plays an important role in computer-aided drug discovery. It is an essential step of virtual screening and drug repositioning. The binding affinity of a drug-target pair is generally expressed in terms of dissociation constant (K_d), inhibition constant (K_i), or the half-maximal inhibitory concentration (IC_{50}). The lower K_d , K_i , or IC_{50} values, the better binding affinities of drug-target pairs. The most commonly used technique to predicting the binding affinity of drug-target pairs is docking simulation, e.g., Glide [1], MOE-Dock [2], AutoDock Vina [3]. However, different docking programs may result in different docking scores for the same drug-target pair [4]. In addition, docking is a computationally expensive and time-consuming process [5], and it can only be applied to proteins whose 3D structures are determined. Therefore, it is difficult to be applied on a large scale. In spite of that, our method only considers the sequence information of the chemical compounds and the proteins, i.e., it does not require the 3D structure information of proteins. Hence, the proposed method is suitable for screening a huge number of drug candidates and target proteins, and it can be easily applied to virtual screening and drug repositioning.

Recently, learning-based algorithms have been developed for drug-target interaction prediction over the last decade. Pahikkala et al. [6] used a Kronecker Regularized Least Squares (KronRLS) method to predict the drug-target interactions based on the chemical structure and protein sequence similarity matrices. He et al. [7] utilized gradient boosting machines called *SimBoost* to predict drug-target binding affinities. Öztürk et al. [8] presented a deep learning-based model called DeepDTA that uses the sequence information of drugs and targets to predict their binding affinities. Shin et al. [9] introduced a new molecule representation based on the self-attention mechanism and a new deep-learning model called Molecule Transformer DTI (MT-DTI) to predict the binding affinities of chemical compounds and proteins. Zhao et al. [10] proposed a deep learning-based end-to-end model named AttentionDTA that uses attention mechanisms on both drug and target sequences to predict their binding affinity scores. Abbasi et al. [11] presented a deep learning-based model called DeepCDA that integrates long short-term memory (LSTM) and convolutional neural network (CNN) to predict drug-target interactions. It is noted that the methods mentioned above are only based on the sequence information of chemical compounds and protein.

In this paper, we propose an ensemble of deep learning models (EnsembleDLM) for drug-target interaction prediction using only sequence information of drug and target. Our contribution is twofold. First, EnsembleDLM has better intra- and inter-domain drug-target interaction prediction performance compared to the sequence-based state-of-the-art methods. Second, we have examined how much data a network needs to achieve a good drug-target interaction prediction performance via transfer learning.

II. MATERIALS AND METHODOLOGY

A. Datasets

1) *Davis*: Davis et al. [12] curated 30,056 K_d binding affinity scores from 68 chemical compounds and 72 kinase inhibitors with 442 kinases. In the Davis dataset, the lower

K_d score indicates the better binding affinity of the drug-target pair.

2) *KIBA*: Tang et al. [13] introduced a model-based approach called Kinase Inhibitor Bio-Activity (KIBA) to integrate three large-scale biochemical assays including IC_{50} , K_i and K_d of kinase inhibitors. The original KIBA dataset provides a total of 246,088 KIBA scores across 52,498 chemical compounds and 467 kinase targets. The lower KIBA score indicates the better binding affinity of the drug-target pair. However, we use the modified KIBA dataset curated by He et al. [7] in this paper. The modified KIBA dataset contains 118,254 drug-target bio-activity scores across 2,111 chemical compounds and 229 kinase targets. The higher modified KIBA score indicates the better binding affinity of the drug-target pair.

3) *ChEMBL*: ChEMBL [14] is an open large-scale bio-activity dataset. In this paper, we curated the interaction of drug-target pairs based on the following criteria in ChEMBL:

- standard_type == "Ki"
- standard_value > 0
- standard_units == "nM"
- standard_relation == "="
- bao_format == "BAO_0000357" (meaning that in the assays, only results with single protein format were considered)

For a drug-target interaction with multiple measurements, the minimum value was taken. In addition, identical values were removed due to duplication. In the end, 137,413 drug-target interactions are curated in our dataset. We then split the curated interactions based on the protein family classification, and remove 894 interactions of unclassified proteins (UP) from the data. The details of splitting the data are described in Table I. In the ChEMBL- K_i dataset, the lower K_i score indicates the better binding affinity of the drug-target pair.

TABLE I
THE DETAILS OF SPLITTING THE CHEMBL DATA INTO FIVE DIFFERENT CLASSES BASED ON THE PROTEIN STRUCTURES. UP : UNCLASSIFIED PROTEINS.

Label	Level-1	Level-2
EK	Enzyme	Kinase
EP	Enzyme	Protease
ER	Epigenetic regulator	Eraser; Reader; Writer
TFNR	Transcription factor	Nuclear receptor
REST	(All interactions) - (EK+EP+ER+TFNR+UP)	

More details of these datasets can be found in Table II.

B. Network Architecture

The network architecture of the individual model is shown in Fig. 1. The network comprises two pathways which are a drug encoder, target encoder, and regressor. Drug encoder and target encoder respectively take a SMILES sequence and a FASTA sequence as an input and output its corresponding feature vector. The drug feature vector is then concatenated

with the target feature vector and feed into the regressor. In the end, the network outputs the predicted binding affinity score of the given drug-target pair. More details of drug pathway, target pathway, and regressor can be found in Table III.

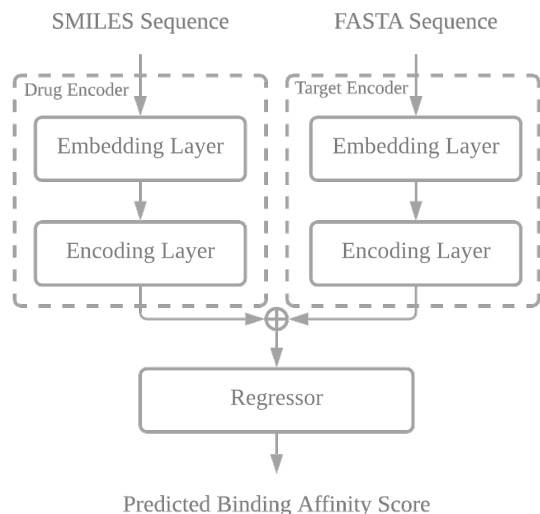


Fig. 1. The network architecture of individual model.

1) *Drug Encoder*: The drug encoder contains an embedding layer and an encoding layer. Three pre-defined embeddings including Morgan fingerprint [15], ErG fingerprint [16], and Daylight fingerprint [17] and one character-based embedding are used in the drug encoder. The one-hot encoder converts the SMILES characters into a binary matrix for the character-based embedding. The encoder layers consist of multiple fully connected layers for the pre-defined embeddings and multiple 1D convolutional layers with one fully connected layer at the end for the character-based embedding.

2) *Target Encoder*: The target encoder also has an embedding layer and an encoding layer. Amino acid composition (AAC) [18] and character-based embedding are used to convert the FASTA sequence into a binary vector. The one-hot encoder converts the FASTA characters into a binary matrix for the character-based embedding. The encoder layers contain multiple fully connected layers for AAC and multiple 1D convolutional layers with one fully connected layer at the end for the character-based embedding.

3) *Regressor*: The regressor begins with a dropout layer [19] with a dropout rate of 0.1 to prevent overfitting followed by multiple fully connected layers. It takes the concatenated feature vector from the drug encoder and target encoder as input and outputs the predicted binding affinity score for the corresponding drug-target pair.

C. Ensemble Modeling

Ensembles have been proven to have better performance than any single model [20] in different applications including

TABLE II
THE DETAILS OF DATASETS CONTAIN THE NUMBER OF UNIQUE DRUGS, THE NUMBER OF UNIQUE TARGETS, THE NUMBER OF INTERACTIONS, BIO-ACTIVITY TYPE, AND STATISTICS OF SMILES SEQUENCE LENGTH AND FASTA SEQUENCE LENGTH.

	# drugs	# targets	# interactions	Bio-activity type	SMILES sequence length			FASTA sequence length		
					Max.	Min.	Avg.	Max.	Min.	Avg.
Davis	68	442	30,056	K_d	92	39	63	2,549	244	789
KIBA	2,111	229	118,254	Mixture of K_d , K_i and IC_{50}	590	20	55	4,128	215	731
ChEMBL-EK	7,330	188	10,508	K_i	417	12	53	4,128	270	957
ChEMBL-EP	21,392	245	34,660	K_i	718	9	70	3,391	99	496
ChEMBL-ER	1,043	53	1,534	K_i	445	12	63	3,046	347	1,051
ChEMBL-REST	47,774	1,116	86,016	K_i	837	3	54	7,078	26	438
ChEMBL-TFNR	2,404	40	3,776	K_i	451	24	63	984	352	677

KIBA is curated by He et al. [7].

TABLE III
THE DETAILS OF NETWORK ARCHITECTURE.

	Drug Pathway				Target Pathway		
	Daylight	ErG	Morgan	CNN	AAC	CNN	Regressor
1 st layer	Linear(2048, 1024)	Linear(315, 1024)	Linear(1024, 1024)	Conv1d(63, 32, 4)	Linear(8420, 1024)	Conv1d(26, 32, 4)	Linear(512, 1024)
2 nd layer	Linear(1024, 256)	Linear(1024, 256)	Linear(1024, 256)	Conv1d(32, 64, 4)	Linear(1024, 256)	Conv1d(32, 64, 4)	Linear(1024, 1024)
3 rd layer	Linear(256, 64)	Linear(256, 64)	Linear(256, 64)	Conv1d(64, 96, 4)	Linear(256, 64)	Conv1d(64, 96, 4)	Linear(1024, 512)
4 th layer	Linear(64, 256)	Linear(64, 256)	Linear(64, 256)	Linear(96, 256)	Linear(64, 256)	Linear(96, 256)	Linear(512, 1)

Linear(X, Y): Linear layer with X input features, Y output features and bias=True.

Conv1D(X, Y, Z): 1D convolutional layer with X input channels, Y input channels, and Z convolving kernel size.

image classification [21], pulmonary tuberculosis diagnosis [22], [23], brain tumor segmentation [24]–[26], solar radiation forecasting [27], [28], and cancer classification [29], [30]. In this paper, we integrate multiple models by taking the arithmetic mean on the predicted binding affinity scores of different models that are defined as

$$\hat{y}_j = \frac{1}{M} \sum_{i=1}^M \bar{y}_{ij}$$

where M is the number of models, and \hat{y}_j and \bar{y}_{ij} is the predicted binding scores of ensemble and individual model i , respectively, for drug-target pair j .

D. Transfer Learning

Transfer learning [31] is the idea of transferring the domain knowledge from previously learned tasks to a new but related task. There are two different methods of transfer learning in neural networks. The first one is to use a pre-trained neural network as a feature extractor and concatenate this feature extractor by one or more fully connected layers. We only train the concatenated fully connected layers with the new data. The second one is to initialize the neural network with pre-trained weights rather than random weights and fine-tune the whole or last few layers with the new data. In this paper, we focus on initializing the network with the pre-trained weights and fine-tuning the whole neural network. Another contribution of this study is to examine how much data does a network needs to

achieve a good drug-target interaction prediction performance via transfer learning.

E. Training and Inference

Training: In this study, we use pK_d for Davis and pK_i for ChEMBL to train the models.

$$pK_d = -\log_{10}\left(\frac{K_d}{10^9}\right) \quad \text{and} \quad pK_i = -\log_{10}\left(\frac{K_i}{10^9}\right)$$

The larger the pK_d and pK_i score, the better the binding affinity of the drug-target pair. In addition, we use the modified KIBA score [7] to train the models. The larger the modified KIBA score, the better the binding affinity of the drug-target pair. During training, models use the Mean Square Error (MSE) as the loss function and adaptive moment estimation (Adam) [32] in the optimization step. The average training time is approximately 0.23 seconds for one iteration with a batch size of 128 on Intel(R) Xeon(R) Platinum 8260 CPU @ 2.40GHz, NVIDIA GeForce RTX 2080 Ti 11GB GDDR6 and 256G DDR4 RAM. The overall pipeline and models are adapted from DeepPurpose [33] with Ax [34].

Hyper-parameter Tuning: Hyper-parameter tuning is an essential step to find a set of optimal hyper-parameters for training a neural network. In this paper, we only focus on tuning the hyper-parameters which determine how the network is trained by utilizing Bayesian optimization [35]. These hyper-parameters include the learning rate searching over $[10^{-6}, 10^{-3}]$, the weight decay searching

over $[0, 0.2]$, the number of training epochs searching over $\{100, 120, 150, 200\}$, and the batch sizes searching over $\{128, 256, 512\}$. The same set of hyper-parameters is used for both training a network from scratch and fine-tuning a network with pre-trained weights.

Inference: In the inference phase, we select the model with the lowest MSE from five-fold cross-validation, and the predicted binding affinity score of a drug-target pair is averaged from seven different models (Daylight-AAC, Morgan-AAC, ErG-AAC, Daylight-CNN, Morgan-CNN, ErG-CNN, and CNN-CNN).

III. EXPERIMENTS AND RESULTS

A. Evaluation Metrics

1) *Mean squared error:* The mean square error (MSE) is used to measure the difference between the predicted binding affinity scores and the ground-truth binding affinity scores, and it is defined as follows:

$$MSE = \frac{1}{N} \sum_{j=1}^N (\hat{y}_j - y_j)^2$$

where N is the number of drug-target pairs, and \hat{y}_j and y_j are the predicted and ground-truth binding affinity scores for the drug-target pair j , respectively. $MSE = 0$ corresponds to the perfect model prediction.

2) *Concordance index:* The concordance index (C-index) [36], which quantifies the quality of rankings, is used to measure the order of the predictions versus the order of the ground truths. The C-index is a value between 1.0 and 0.0. A value of 1.0 indicates a perfect separation of drug-target pairs with different binding affinity scores and a value of 0.5 indicates no predictive discrimination.

3) *Pearson correlation coefficient:* The Pearson correlation coefficient (PCC) [37] provides a measure of the strength of linear association between the predicted and ground-truth binding affinity scores. Given a pair of binding affinity scores (\hat{Y}, Y) , their Pearson correlation coefficient $\rho_{\hat{Y}, Y}$ is:

$$\rho_{\hat{Y}, Y} = \frac{cov(\hat{Y}, Y)}{\sigma_{\hat{Y}} \sigma_Y}$$

where $\sigma_{\hat{Y}}$ and σ_Y are the standard deviations of the predicted and ground-truth binding affinity scores, respectively, and cov is the co-variance. The range of the Pearson correlation coefficient is between 1.0 and -1.0. 1.0, -1.0, and 0.0 indicate a strong positive, strong negative, and zero correlation, respectively, between predicted and ground-truth binding affinity scores.

B. Single model vs. ensemble modeling

In this section, we would like to examine the performance of each model with different drug-target encoder combinations and compare their performance with the proposed ensemble modeling approach on the Davis, KIBA, and ChEMBL-REST datasets. The proposed ensemble of deep learning models

(EnsembleDLM) contains the Daylight-AAC model, Morgan-AAC model, ErG-AAC model, Daylight-CNN model, Morgan-CNN model, ErG-CNN model, and CNN-CNN model. We first leave 20% of the data (6,012 interactions for Davis, 23,651 interactions for KIBA, and 17,190 interactions for ChEMBL-REST) out for the test. Then, we implement the five-fold cross-validation within the remaining data (24,044 interactions for Davis, 94,603 interactions for KIBA, and 68,759 interactions for ChEMBL-REST). The remaining data is equally split into five subsets. Each subset is then taken in turn as a validation set, and the remaining four sets are used to train the model. Cross-validation is used to prevent over-fitting [38]. The performance of each model and proposed EnsembleDLM on the validation set and test set of Davis and KIBA are presented in Table IV and ChEMBL-REST is presented in Table V.

C. Compared to the state-of-the-art models

In this section, we compare the performance of our proposed approach with other state-of-the-art models. It is noted that for a fair comparison, we only compare our proposed approach with the sequence-based models, i.e., the inputs to the model are SMILES sequence and FASTA sequence. Davis and KIBA are used to compare the performance of different methods. We also withhold 20% of the data for the test and perform five-fold cross-validation on the remaining data. The comparisons of our approach and the state-of-the-art approaches are shown in Table VI for Davis and Table VII for KIBA.

D. Cross-domain Drug-Target Interaction Prediction via Fine-Tuning

In this section, we would like to examine the cross-domain drug-target interaction prediction performance of EnsembleDLM between different datasets including Davis, KIBA, and Ki-ChEMBL. For different types of models, we select the best one from five-fold cross-validation in the original domain. We then fine-tune each selected model with the original hyper-parameter set to the new domain using different portions of data, i.e., the Bayesian optimization is not used at this time. It is noted that all layers of drug encoder, target encoder, and regressor are fine-tuned. In the end, the output of our fine-tuned EnsembleDLM is the average predictions of seven fine-tuned models.

1) *Same protein class with different binding affinity scores:* In this experiment, we would like to examine the performance of EnsembleDLM across different binding affinity scores in the same protein class. Davis and KIBA are used in this experiment. Davis consists of K_d interactions of enzyme inhibitions, and KIBA combines K_d , K_i , and IC_{50} interactions of enzyme inhibitions into a new score. We hold 20% of new domain data for the test, and the remaining 80% of new domain data are the training data. We use different portions (1%, 25%, 50%, 75%, 100%) of training data to fine-tune the EnsembleDLM and compare its performance with DeepDTA [8] and DeepCDA [11]. We implement five-fold cross-validation on the training set. The results are presented in Table VIII.

TABLE IV

THE COMPARISON OF OUR PROPOSED APPROACH AND EACH INDIVIDUAL MODEL ON THE VALIDATION SET AND TEST SET OF DAVIS AND KIBA WITH 5-FOLD CROSS-VALIDATION. THE INDIVIDUAL MODEL IS REPRESENTED BY (DRUG ENCODER)-(TARGET ENCODER). THE BOLD NUMBER HIGHLIGHTS THE BEST PERFORMANCE. THE RESULTS ARE ROUNDED DOWN TO THREE DECIMAL PLACES.

Drug-Target	Davis				KIBA			
	Validation		Test		Validation		Test	
	MSE±std	C-index±std	MSE±std	C-index±std	MSE±std	C-index±std	MSE±std	C-index±std
Daylight-AAC	0.256±0.011	0.875±0.006	0.251±0.003	0.874±0.001	0.170±0.012	0.874±0.002	0.168±0.003	0.877±0.002
Morgan-AAC	0.268±0.012	0.871±0.006	0.256±0.008	0.875±0.004	0.178±0.004	0.875±0.001	0.175±0.003	0.877±0.003
ErG-AAC	0.261±0.024	0.874±0.013	0.253±0.006	0.879±0.001	0.194±0.005	0.869±0.002	0.188±0.003	0.868±0.003
Daylight-CNN	0.251±0.005	0.880±0.006	0.249±0.007	0.876±0.005	0.174±0.005	0.876±0.003	0.168±0.005	0.877±0.003
Morgan-CNN	0.244±0.012	0.881±0.006	0.234±0.004	0.881±0.005	0.171±0.003	0.880±0.003	0.169±0.004	0.881±0.003
ErG-CNN	0.243±0.010	0.883±0.006	0.242±0.011	0.881±0.004	0.194±0.006	0.869±0.003	0.187±0.004	0.869±0.004
CNN-CNN	0.250±0.008	0.882±0.006	0.237±0.003	0.883±0.005	0.184±0.009	0.868±0.005	0.181±0.005	0.868±0.006
Proposed approach	0.202±0.006	0.907±0.004	0.204±0.002	0.905±0.001	0.138±0.003	0.895±0.001	0.138±0.003	0.896±0.001

TABLE V

THE COMPARISON OF OUR PROPOSED APPROACH AND EACH INDIVIDUAL MODEL ON THE VALIDATION SET AND TEST SET OF ChEMBL-REST WITH 5-FOLD CROSS-VALIDATION. THE INDIVIDUAL MODEL IS REPRESENTED BY (DRUG ENCODER)-(TARGET ENCODER). THE BOLD NUMBER HIGHLIGHTS THE BEST PERFORMANCE. THE RESULTS ARE ROUNDED DOWN TO THREE DECIMAL PLACES.

Drug-Target	ChEMBL-REST			
	Validation		Test	
	MSE±std	C-index±std	MSE±std	C-index±std
Daylight-AAC	0.868±0.060	0.820±0.003	0.830±0.017	0.820±0.003
Morgan-AAC	0.848±0.040	0.822±0.004	0.815±0.037	0.823±0.003
ErG-AAC	0.937±0.072	0.813±0.003	0.884±0.028	0.812±0.003
Daylight-CNN	0.905±0.076	0.815±0.004	0.865±0.024	0.815±0.005
Morgan-CNN	0.855±0.068	0.822±0.002	0.823±0.028	0.821±0.004
ErG-CNN	0.919±0.032	0.814±0.002	0.878±0.018	0.811±0.003
CNN-CNN	0.925±0.075	0.809±0.002	0.894±0.019	0.809±0.002
Proposed approach	0.636±0.035	0.845±0.002	0.638±0.008	0.845±0.001

TABLE VI

THE COMPARISON OF OUR APPROACH AND THE STATE-OF-THE-ART APPROACHES WITH 5-FOLD CROSS-VALIDATION ON THE DAVIS DATASET. THE BOLD NUMBER HIGHLIGHTS THE BEST PERFORMANCE. THE RESULTS ARE ROUNDED DOWN TO THREE DECIMAL PLACES.

Models	MSE(±std)	C-index±std
KronRLS [6]	0.379	0.782±0.001
SimiBoost [7]	0.282	0.836±0.001
DeepDTA [8]	0.261	0.863±0.002
MT-DTI [9]	0.245	0.882±0.001
AttentionDTA [10]	0.216±0.019	0.882±0.004
DeepCDA [11]	0.248	0.889±0.002
Proposed approach	0.202±0.006	0.907±0.004

TABLE VII

THE COMPARISON OF OUR APPROACH AND STATE-OF-THE-ART APPROACHES WITH 5-FOLD CROSS-VALIDATION ON THE KIBA DATASET. THE BOLD NUMBER HIGHLIGHTS THE BEST PERFORMANCE. THE RESULTS ARE ROUNDED DOWN TO THREE DECIMAL PLACES.

Models	MSE(±std)	C-index±std
KronRLS [6]	0.411	0.782±0.001
SimiBoost [7]	0.222	0.836±0.001
DeepDTA [8]	0.194	0.863±0.002
MT-DTI [9]	0.152	0.882±0.001
AttentionDTA [10]	0.155±0.003	0.882±0.004
DeepCDA [11]	0.176	0.889±0.002
Proposed approach	0.138±0.003	0.895±0.001

2) *Different protein classes with same binding affinity score:* We then evaluate the performance of EnsembleDLM

across different protein classes with the same binding affinity score. The ChEMBL-REST dataset is used as the original

TABLE VIII

THE CROSS-DOMAIN PERFORMANCE COMPARISONS OF OUR APPROACH AND STATE-OF-THE-ART APPROACHES ON DAVIS AND KIBA. THE RESULTS ARE ROUNDED DOWN TO TWO DECIMAL PLACES.

	Davis \rightarrow KIBA				KIBA \rightarrow Davis			
	Validation		Test		Validation		Test	
	C-index \pm std	PCC \pm std						
DeepDTA [8]	0.55 \pm 0.01	-	-	-	0.67 \pm 0.04	-	-	-
DeepCDA [11]	0.58 \pm 0.01	-	-	-	0.68 \pm 0.03	-	-	-
Proposed Approach	0.59\pm0.01	0.32 \pm 0.01	0.59 \pm 0.00	0.32 \pm 0.01	0.73\pm0.01	0.52 \pm 0.02	0.73 \pm 0.01	0.52 \pm 0.01
DeepDTA [8] with DA	0.60 \pm 0.04	-	-	-	0.72 \pm 0.04	-	-	-
DeepCDA [11] with DA	0.64 \pm 0.03	-	-	-	0.74 \pm 0.03	-	-	-
Proposed Approach with TL (1%)	0.71 \pm 0.01	0.53 \pm 0.01	0.71 \pm 0.01	0.53 \pm 0.01	0.75 \pm 0.01	0.53 \pm 0.02	0.76 \pm 0.01	0.54 \pm 0.01
Proposed Approach with TL (25%)	0.85 \pm 0.00	0.84 \pm 0.00	0.85 \pm 0.00	0.84 \pm 0.00	0.87 \pm 0.01	0.79 \pm 0.00	0.87 \pm 0.00	0.78 \pm 0.01
Proposed Approach with TL (50%)	0.87 \pm 0.00	0.87 \pm 0.00	0.87 \pm 0.00	0.87 \pm 0.00	0.89 \pm 0.00	0.84 \pm 0.01	0.89 \pm 0.00	0.83 \pm 0.00
Proposed Approach with TL (75%)	0.88 \pm 0.00	0.89 \pm 0.00	0.88 \pm 0.00	0.89\pm0.00	0.90 \pm 0.00	0.86 \pm 0.01	0.90\pm0.00	0.85 \pm 0.00
Proposed Approach with TL (100%)	0.89\pm0.00	0.90\pm0.00	0.89\pm0.00	0.89\pm0.00	0.91\pm0.00	0.87\pm0.01	0.90\pm0.00	0.86\pm0.00

DA: domain adaptation. TL: transfer learning.

domain, and the EnsembleDLM is fine-tuned to new domains (ChEMBL-ER, ChEMBL-TFNR, ChEMBL-EK, and ChEMBL-EP). These datasets only contain the K_i drug-target interactions. The protein classes in the ChEMBL-ER, ChEMBL-TFNR, ChEMBL-EK and ChEMBL-EP sets are excluded in the ChEMBL-REST set. We first divide 20% of new domain data for test and 80% of new domain data for training. We then use different portions (1%, 25%, 50%, 75%, 100%) of new domain training data to fine-tune the base EnsembleDLM with five-fold cross-validation. The results are presented in Table IX.

3) *Different protein classes with different binding affinity scores*: In this experiment, we would like to examine the cross-domain performance of EnsembleDLM across different protein classes with different binding affinity scores. ChEMBL-REST is used as the base (original) domain. It contains only K_i interaction of drug-target pairs, and the interactions of the kinase are not included in this set. The KIBA and Davis datasets are used as new domains. KIBA comprises $KIBA$ scores from the interactions of kinase, and the KIBA score is integrated by IC_{50} , K_d , and K_i . Davis consists of K_d interactions of drugs and kinase. We left 20% of new domain data for the test, and 80% of the remaining new domain data are the training data. EnsembleDLM is first trained by interactions of the base domain (ChEMBL-REST) and then fine-tuned to the new domain (KIBA, Davis) by using different portions (1%, 25%, 50%, 75%, 100%) of new domain training interactions. The results are shown in Table X

IV. DISCUSSION AND CONCLUSION

We first demonstrate that EnsembleDLM has better performance than any single model within EnsembleDLM and the sequence-based state-of-the-art methods. From Table IV and V, EnsembleDLM has a remarkable improvement compared to any single model within the EnsembleDLM in Davis, KIBA, and ChEMBL-REST datasets. It also has the smallest standard

deviations compared to other single models. Compared to the best model (Morgan-CNN) within the EnsembleDLM, EnsembleDLM has approximately 17.21% and 2.95% improvements on the MSE and CI in Davis validation sets, and 12.82% and 2.72% improvements on the MSE and CI in Davis test set, respectively. It also has approximately 19.3% and 1.7% improvements on the MSE and CI in KIBA validation sets, and 18.34% and 1.7% improvements on the MSE and CI in the KIBA test set, respectively, compared to the best model (Morgan-CNN) within the EnsembleDLM. Moreover, EnsembleDLM has approximately 25% and 2.8% improvements on the MSE and CI in ChEMBL-REST validation sets, and 21.72% 2.67% improvements on the MSE and CI in ChEMBL-REST test set, respectively, compared to the best model (Morgan-AAC) within the EnsembleDLM. From Table VI and VII, EnsembleDLM has the best performance compared to the state-of-the-art methods in both Davis and KIBA datasets. It is noted that we only compare to the sequence-based methods for a fair comparison.

To evaluate the cross-domain performance of EnsembleDLM, we come up with three different scenarios: 1.) same protein class with different bio-activity types, 2.) different protein classes with the same bio-activity type, and 3.) different protein classes with different bio-activity types. Davis and KIBA datasets are used for the case of the same protein class with different bio-activity types. They comprise kinase inhibitors bio-activity data but with different bio-activity types (K_d for Davis and $KIBA$ for KIBA). Davis and KIBA datasets have 9 overlapping drugs and 179 overlapping targets. From Table VIII, EnsembleDLM has better cross-domain drug-target interaction prediction performance compared to the state-of-the-art methods without transfer learning or domain adaptation in both Davis \rightarrow KIBA and KIBA \rightarrow Davis. With only 1% transfer learning data, EnsembleDLM has better performance than the state-of-the-art methods with domain adaptation in both Davis \rightarrow KIBA and KIBA \rightarrow Davis. With 100% transfer

TABLE IX

THE CROSS-DOMAIN PERFORMANCE OF OUR APPROACH ON K_i INTERACTIONS OF ChEMBL DATASET BETWEEN DIFFERENT PROTEIN CLASSES WITH 5-FOLD CROSS-VALIDATION. DIFFERENT SIZES OF NEW DOMAIN DATA ARE USED TO FINE-TUNE THE BASE ENSEMBLEDLM. THE RESULTS ARE ROUNDED DOWN TO TWO DECIMAL PLACES, AND THE BOLD NUMBER HIGHLIGHTS THE BEST PERFORMANCE.

ChEMBL								
Size	REST → ER		REST → TFNR		REST → EK		REST → EP	
	PCC±std	C-index±std	PCC±std	C-index±std	PCC±std	C-index±std	PCC±std	C-index±std
0%	0.148±0.081	0.550±0.027	-0.016±0.051	0.504±0.016	0.263±0.022	0.589±0.008	0.225±0.026	0.578±0.007
1%	0.391±0.074	0.638±0.024	0.304±0.059	0.601±0.016	0.608±0.022	0.714±0.009	0.442±0.023	0.656±0.006
25%	0.776±0.026	0.799±0.013	0.774±0.014	0.789±0.007	0.843±0.005	0.827±0.001	0.836±0.006	0.829±0.003
50%	0.828±0.030	0.828±0.016	0.824±0.011	0.817±0.006	0.871±0.005	0.846±0.001	0.866±0.002	0.850±0.003
75%	0.849±0.019	0.843±0.008	0.846±0.008	0.831±0.004	0.885±0.005	0.857±0.001	0.878±0.002	0.861±0.003
100%	0.860±0.017	0.849±0.008	0.854±0.006	0.836±0.004	0.891±0.004	0.862±0.001	0.883±0.003	0.866±0.002

TABLE X

THE CROSS-DOMAIN PERFORMANCE COMPARISONS OF ENSEMBLEDLM. THE ENSEMBLEDLM IS FIRST TRAINED BY WHOLE DATA OF ChEMBL-REST SET, AND THEN FINE-TUNED TO DAVIS AND KIBA SET USING DIFFERENT PORTIONS OF NEW DOMAIN DATA. THE RESULTS ARE ROUNDED DOWN TO TWO DECIMAL PLACES.

	ChEMBL-REST → KIBA				ChEMBL-REST → Davis			
	Validation		Test		Validation		Test	
	C-index±std	PCC±std	C-index±std	PCC±std	C-index±std	PCC±std	C-index±std	PCC±std
Proposed Approach without TL	0.54±0.01	0.12±0.03	0.54±0.01	0.12±0.02	0.51±0.02	0.03±0.02	0.52±0.02	0.04±0.003
Proposed Approach with TL (1%)	0.67±0.00	0.47±0.01	0.67±0.00	0.46±0.01	0.72±0.02	0.43±0.02	0.73±0.01	0.44±0.02
Proposed Approach with TL (25%)	0.84±0.00	0.82±0.00	0.84±0.00	0.82±0.00	0.86±0.01	0.77±0.01	0.86±0.00	0.76±0.00
Proposed Approach with TL (50%)	0.88±0.00	0.87±0.00	0.88±0.00	0.87±0.00	0.89±0.00	0.82±0.01	0.89±0.00	0.81±0.01
Proposed Approach with TL (75%)	0.89±0.00	0.89±0.00	0.89±0.00	0.89±0.00	0.90±0.01	0.85±0.01	0.90±0.00	0.84±0.00
Proposed Approach with TL (100%)	0.90±0.00	0.90±0.00	0.90±0.00	0.90±0.00	0.91±0.00	0.86±0.01	0.90±0.00	0.85±0.00

TL: transfer learning.

learning data, EnsembleDLM approaches similar performance compared to the training-from-scratch EnsembleDLM shown in Table IV. Bayesian optimization is not applied for hyperparameter searching in the transfer learning phase. Therefore, the performance of the training-from-scratch EnsembleDLM is marginally better than the performance of the transfer-learning EnsembleDLM. Then, ChEMBL datasets are used to evaluate the cross-domain performance of EnsembleDLM for the case of different protein classes with the same bio-activity type. Table IX shows that without the transfer learning, EnsembleDLM has the best performance on the EK dataset and the worst performance on the TFNR dataset. With approximately 25% transfer learning data, EnsembleDLM has a good (PCC and C-index > 0.8) performance in EK and EP datasets. EnsembleDLM also has a good (PCC and C-index > 0.8) performance in ER and TFNR datasets with approximately 50% transfer learning data. With 100% transfer learning data, the EnsembleDLM again has the best performance on the EK dataset followed by EP, ER, and TFNR dataset. In the last scenario, we would like to evaluate the cross-domain performance of our model across different protein families with different bio-activity types. ChEMBL-REST is used as the base (original) dataset, and KIBA and Davis

are used as new domain datasets. KIBA and Davis contain interactions of kinases that are not curated in the ChEMBL-REST set. The bio-activity type of ChEMBL-REST is K_i , whereas the bio-activity type is K_d and KIBA for the Davis and KIBA dataset, respectively. Different portions (1%, 25%, 50%, 75%, and 100%) of data from new domains are used for transfer learning. Table X shows that without transfer learning, EnsembleDLM has better performance in ChEMBL-REST → KIBA. With approximately 25% transfer learning data, EnsembleDLM has a good (PCC and C-index > 0.8) performance in both ChEMBL-REST → KIBA and ChEMBL-REST → Davis. With 100% transfer learning data, EnsembleDLM has similar performance no matter the base (original) datasets are from the same protein class (Davis → KIBA and KIBA → Davis) or the different protein classes (ChEMBL-REST → KIBA and ChEMBL-REST → Davis). However, for different protein families analysis, EnsembleDLM has better performance for the same bio-activity type (ChEMBL-REST → ChEMBL-EK) than different bio-activity types (ChEMBL-REST → KIBA and ChEMBL-REST → Davis).

In conclusion, EnsembleDLM achieves better performance compared to any single model within the EnsembleDLM and the sequence-based state-of-the-art methods. It also has better

cross-domain performance compared to the sequence-based state-of-the-art methods. With approximately 50% transfer learning data, i.e., the training set has twice as much data as the test set, EnsembleDLM achieves a good performance (PCC and C-index > 0.8) in the new domain in every scenario. However, the EnsembleDLM only has marginal improvements from 50% to 75% of transfer learning data and from 75% to 100% of transfer learning data.

ACKNOWLEDGMENT

We would like to thank Kexin Huang and Tianfan Fu for technical support on DeepPurpose, Dr. Karim Abbasi for his assistance on DeepCDA, and Taiwan Computing Cloud (TWCC) for computational resources.

REFERENCES

- R. A. Friesner, J. L. Banks, R. B. Murphy, T. A. Halgren, J. J. Klicic, D. T. Mainz, M. P. Repasky, E. H. Knoll, M. Shelley, J. K. Perry *et al.*, "Glide: a new approach for rapid, accurate docking and scoring. 1. method and assessment of docking accuracy," *Journal of medicinal chemistry*, vol. 47, no. 7, pp. 1739–1749, 2004.
- S. Vilar, G. Cozza, and S. Moro, "Medicinal chemistry and the molecular operating environment (moe): application of qsar and molecular docking to drug discovery," *Current topics in medicinal chemistry*, vol. 8, no. 18, pp. 1555–1572, 2008.
- O. Trott and A. J. Olson, "Autodock vina: improving the speed and accuracy of docking with a new scoring function, efficient optimization, and multithreading," *Journal of computational chemistry*, vol. 31, no. 2, pp. 455–461, 2010.
- Z. Wang, H. Sun, X. Yao, D. Li, L. Xu, Y. Li, S. Tian, and T. Hou, "Comprehensive evaluation of ten docking programs on a diverse set of protein–ligand complexes: the prediction accuracy of sampling power and scoring power," *Physical Chemistry Chemical Physics*, vol. 18, no. 18, pp. 12964–12975, 2016.
- N. M. Hassan, A. A. Alhossary, Y. Mu, and C.-K. Kwoh, "Protein–ligand blind docking using quickvina-w with inter-process spatio-temporal integration," *Scientific reports*, vol. 7, no. 1, pp. 1–13, 2017.
- T. Pahikkala, A. Airola, S. Pietilä, S. Shakyawar, A. Szwajda, J. Tang, and T. Aittokallio, "Toward more realistic drug–target interaction predictions," *Briefings in bioinformatics*, vol. 16, no. 2, pp. 325–337, 2015.
- T. He, M. Heidemeyer, F. Ban, A. Cherkasov, and M. Ester, "Simboost: a read-across approach for predicting drug–target binding affinities using gradient boosting machines," *Journal of cheminformatics*, vol. 9, no. 1, pp. 1–14, 2017.
- H. Öztürk, A. Özgür, and E. Ozkirimli, "Deepdta: deep drug–target binding affinity prediction," *Bioinformatics*, vol. 34, no. 17, pp. i821–i829, 2018.
- B. Shin, S. Park, K. Kang, and J. C. Ho, "Self-attention based molecule representation for predicting drug–target interaction," in *Machine Learning for Healthcare Conference*. PMLR, 2019, pp. 230–248.
- Q. Zhao, F. Xiao, M. Yang, Y. Li, and J. Wang, "Attentiondta: prediction of drug–target binding affinity using attention model," in *2019 IEEE International Conference on Bioinformatics and Biomedicine (BIBM)*. IEEE, 2019, pp. 64–69.
- K. Abbasi, P. Razzaghi, A. Poso, M. Amanlou, J. B. Ghasemi, and A. Masoudi-Nejad, "Deepcda: deep cross-domain compound–protein affinity prediction through lstm and convolutional neural networks," *Bioinformatics*, vol. 36, no. 17, pp. 4633–4642, 2020.
- M. I. Davis, J. P. Hunt, S. Hergard, P. Ciceri, L. M. Wodicka, G. Palares, M. Hocker, D. K. Treiber, and P. P. Zarrinkar, "Comprehensive analysis of kinase inhibitor selectivity," *Nature biotechnology*, vol. 29, no. 11, pp. 1046–1051, 2011.
- J. Tang, A. Szwajda, S. Shakyawar, T. Xu, P. Hintsanen, K. Wennerberg, and T. Aittokallio, "Making sense of large-scale kinase inhibitor bioactivity data sets: a comparative and integrative analysis," *Journal of Chemical Information and Modeling*, vol. 54, no. 3, pp. 735–743, 2014.
- A. Gaulton, A. Hersey, M. Nowotka, A. P. Bento, J. Chambers, D. Mendez, P. Mutowo, F. Atkinson, L. J. Bellis, E. Cibrián-Uhalte *et al.*, "The chEMBL database in 2017," *Nucleic acids research*, vol. 45, no. D1, pp. D945–D954, 2017.
- D. Rogers and M. Hahn, "Extended-connectivity fingerprints," *Journal of chemical information and modeling*, vol. 50, no. 5, pp. 742–754, 2010.
- N. Stiefl, I. A. Watson, K. Baumann, and A. Zaliani, "Erg: 2d pharmacophore descriptions for scaffold hopping," *Journal of chemical information and modeling*, vol. 46, no. 1, pp. 208–220, 2006.
- I. Daylight Chemical Information Systems, "Daylight," online; accessed 06 April 2021. [Online]. Available: <https://www.daylight.com/>
- M. H. Smith, "The amino acid composition of proteins," *Journal of Theoretical Biology*, vol. 13, pp. 261–282, 1966.
- N. Srivastava, G. Hinton, A. Krizhevsky, I. Sutskever, and R. Salakhutdinov, "Dropout: a simple way to prevent neural networks from overfitting," *The journal of machine learning research*, vol. 15, no. 1, pp. 1929–1958, 2014.
- T. G. Dietterich, "Ensemble methods in machine learning," in *International workshop on multiple classifier systems*. Springer, 2000, pp. 1–15.
- K. He, X. Zhang, S. Ren, and J. Sun, "Deep residual learning for image recognition," in *Proceedings of the IEEE conference on computer vision and pattern recognition*, 2016, pp. 770–778.
- P. Lakhani and B. Sundaram, "Deep learning at chest radiography: automated classification of pulmonary tuberculosis by using convolutional neural networks," *Radiology*, vol. 284, no. 2, pp. 574–582, 2017.
- E. Alves, J. B. Souza Filho, and A. L. Kritski, "An ensemble approach for supporting the respiratory isolation of presumed tuberculosis inpatients," *Neurocomputing*, vol. 331, pp. 289–300, 2019.
- K. Kamnitsas, W. Bai, E. Ferrante, S. McDonagh, M. Sinclair, N. Pawlowski, M. Rajchl, M. Lee, B. Kainz, D. Rueckert *et al.*, "Ensembles of multiple models and architectures for robust brain tumour segmentation," in *International MICCAI brainlesion workshop*. Springer, 2017, pp. 450–462.
- P.-Y. Kao, T. Ngo, A. Zhang, J. W. Chen, and B. Manjunath, "Brain tumor segmentation and tractographic feature extraction from structural mr images for overall survival prediction," in *International MICCAI Brainlesion Workshop*. Springer, 2018, pp. 128–141.
- P.-Y. Kao, F. Shailja, J. Jiang, A. Zhang, A. Khan, J. W. Chen, and B. Manjunath, "Improving patch-based convolutional neural networks for mri brain tumor segmentation by leveraging location information," *Frontiers in neuroscience*, vol. 13, p. 1449, 2020.
- C. Voyant, G. Notton, S. Kalogirou, M.-L. Nivet, C. Paoli, F. Motte, and A. Fouilly, "Machine learning methods for solar radiation forecasting: A review," *Renewable Energy*, vol. 105, pp. 569–582, 2017.
- M. Guermoui, F. Melgani, K. Gairaa, and M. L. Mekhalfi, "A comprehensive review of hybrid models for solar radiation forecasting," *Journal of Cleaner Production*, vol. 258, p. 120357, 2020.
- A. C. Tan and D. Gilbert, "Ensemble machine learning on gene expression data for cancer classification," *Applied bioinformatics*, vol. 2, no. 3 Suppl, pp. S75–S83, 2003.
- H. Liu, L. Liu, and H. Zhang, "Ensemble gene selection for cancer classification," *Pattern Recognition*, vol. 43, no. 8, pp. 2763–2772, 2010.
- S. J. Pan and Q. Yang, "A survey on transfer learning," *IEEE Transactions on knowledge and data engineering*, vol. 22, no. 10, pp. 1345–1359, 2009.
- D. P. Kingma and J. Ba, "Adam: A method for stochastic optimization," *arXiv preprint arXiv:1412.6980*, 2014.
- K. Huang, T. Fu, L. M. Glass, M. Zitnik, C. Xiao, and J. Sun, "Deep-purpose: a deep learning library for drug–target interaction prediction," *Bioinformatics*, 2020.
- E. Bakshy, L. Dworkin, B. Karrer, K. Kashin, B. Letham, A. Murthy, and S. Singh, "Ae: A domain-agnostic platform for adaptive experimentation," in *Workshop on System for ML*, 2018.
- J. Snoek, H. Larochelle, and R. P. Adams, "Practical bayesian optimization of machine learning algorithms," *Advances in Neural Information Processing Systems*, 2012.
- F. E. Harrell Jr, K. L. Lee, and D. B. Mark, "Multivariable prognostic models: issues in developing models, evaluating assumptions and adequacy, and measuring and reducing errors," *Statistics in medicine*, vol. 15, no. 4, pp. 361–387, 1996.
- J. Benesty, J. Chen, Y. Huang, and I. Cohen, "Pearson correlation coefficient," in *Noise reduction in speech processing*. Springer, 2009, pp. 1–4.
- A. Y. Ng *et al.*, "Preventing" overfitting" of cross-validation data," in *ICML*, vol. 97. Citeseer, 1997, pp. 245–253.